P2E.1 GPS Dropwindsonde Observations of Tropical Cyclone Low-level Wind Maxima

Ian M. Giammanco*[1], John L. Schroeder[1], Mark D. Powell[2] and Douglas A. Smith[1]
[1]Texas Tech University, Lubbock, Texas
[2] NOAA/AOML Hurricane Research Division, Miami, Florida

1. Introduction

Within the last decade substantial improvements have been made in one's ability to observe the tropical cyclone boundary layer. The implementation of the GPS dropwindsonde (GPS sonde) in 1997 has provided glimpses into the complex nature of the flow in this region (Hock and Franklin 1999). Sonde observations have revealed the presence of low-level wind maxima at heights well below 1 km and similar structure to the classic nocturnal low-level jet (Franklin et al. 2003; Powell et al. 2003). Modeling studies by Kepert (2001) and Kepert and Wang (2001) have been successful in reproducing similar vertical profiles and evaluating the jets departure from the gradient wind. However, individual observed wind profiles, shown in Figure 1 and Figure 2, exhibit a more complex structure. (Franklin et al. 2003; Kepert 2006 Pt. I and Pt. II).

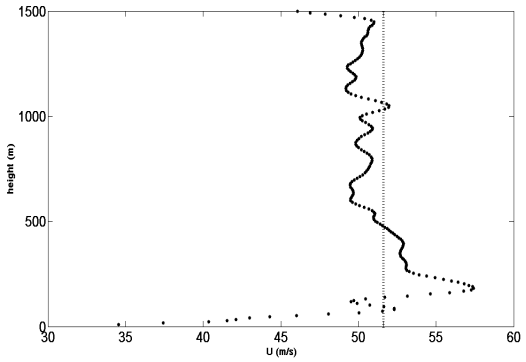

Figure 1. GPS sonde profile from Hurricane Bonnie 23 August 1998, released at 2148 UTC. Dashed line represents the mean boundary layer wind speed (MBL; Franklin et al. 2003).

*Corresponding author address: Ian Giammanco, Wind Science and Engineering Research Center, Texas Tech University, Lubbock TX 79409. ian.giammanco@ttu.edu

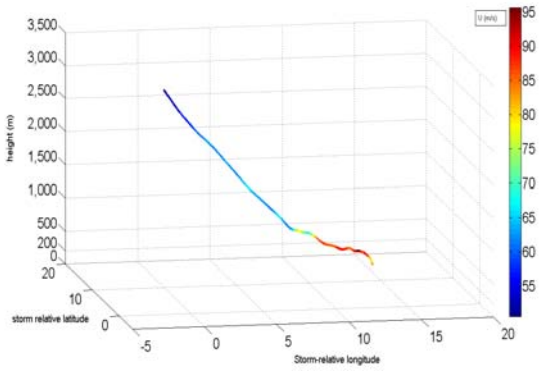

Figure 2. 3-D plot of a sonde decent from Hurricane Rita, 21 September 2005 at 0313 UTC. The horizontal axes are storm-relative latitude and longitude. The sonde decent is color coded by wind speed (ms^{-1}).

The GPS sonde has provide a wealth of new data available for analyses. Given the substantial quantity of profiles now available, a more comprehensive study of low-level wind maxima can be conducted. The jet-like features also represent momentum potentially available for vertical transport. Low-level wind maxima have been identified at altitudes below 200 m within 11% of all GPS sondes. The rapid change in wind speed with height associated with their presence could result in the upper floors of high-rise structures (height > 30 m) experiencing wind above their minimum design standards for intense tropical cyclones. However, there is currently little information available to evaluate the presence of low-level wind maxima in landfalling hurricanes. Knupp et al. (2006) has shown some observational evidence of low-level jet features at altitudes near 500 m in two weak landfalling tropical cyclones. The sharp increase in wind speed above the surface may not be well captured by log and power law wind profiles. Although there is little data to examine the jet features strictly at landfall, their presence in open-ocean conditions suggested that the feature cannot be ignored.

2. Data

Over 2000 GPS sondes have been post-processed and archived by NOAA/AOML Hurricane Research Division from both the Atlantic and Eastern Pacific basins. The data were reduced by only including GPS sondes which were released between 5 – 200 km radii from the cyclone center. The available sondes were then grouped by MBL wind speed, similar to Powell et al. (2003). The sonde contains a summary statistics file as well as the post-processed 2 Hz data from the sonde release. Datasets of both summary statistics and high-resolution sonde data were created using a Java-based query application which accesses the sonde archive, at NOAA/AOML/Hurricane Research Division.

Additional data was incorporated with the sonde datasets. The HURDAT database and accompanying best-track data were used to assign an intensification category to each GPS sonde profile using a minimum central pressure trend, for a 24 hour time window centered on the sonde launch. Table 1 provides the categories, along with the number of sondes included in each one. The rapid intensification criterion of a pressure fall of 28 hPa over a 24 hour period was based on results from DeMaria and Kaplan (1999) for rapidly intensifying tropical cyclones in the Atlantic Hurricane Basin. An environmental shear magnitude will also be assigned to each sonde. Shear will be computed using the method specified by DeMaria and Kaplan (1994). However, this data has not yet been processed and has not been assimilated into the dataset.

Table 1. Cyclone intensification trend categories. Rapidly intensifying category based on DeMaria and Kaplan (1999).

Intensity trend category	**24 hour pressure trend**	**Number of sondes**
Weakening	Increase > 6 hPa	289
Steady-state	Change ± 5 hPa	691
Intensifying	Decrease 6 – 27 hPa	200
Rapidly Intensifying	Decrease > 28 hPa	89

3. Preliminary analysis of wind maxima

The preliminary analysis conducted on the dataset focused on characterizing the maximum wind speed (U_{max}) found within the individual wind profiles. Sondes were grouped by MBL using 10 ms^{-1} bins, as used by Powell et al. (2003). An emphasis was placed on examining sondes with U_{max} located below 200 m in altitude. As expected, a large percentage (72%) of sondes contained a maximum wind speed below 1 km and 11% contained a maximum below 200 m. The mean height and standard deviation of the wind maximum decreased with increasing MBL, as well as the standard deviation, shown in Table 2. It is noted that 91% of all sondes collected data below 100 m. The distribution of the height of the maximum wind speed is shown in Figure 3.

Table 2. Summary of all GPS sondes (5 - 200 km radii).

MBL Group (ms^{-1})	Mean height U_{max} (m)	σ U_{max} height (m)	% of sondes with U_{max} below 500 m	% of sondes with U_{max} below 200 m
10 – 19.999	1703.0	2308.0	27%	8%
20 – 29.999	1403.2	1521.1	27%	7%
30 – 39.999	867.4	778.4	37%	11%
40 – 49.999	758.4	568.2	41%	11%
50 – 59.999	550.3	436.7	58%	13%
60 – 69.999	526.9	400.3	61%	11%
70 – 79.999	453.3	300.8	92%	11%
80 – 89.999	488.7	293.2	61%	7%

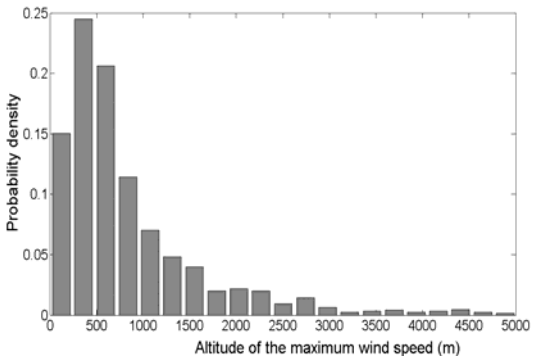

Figure 3. Frequency distribution of the height of the maximum wind speed. Bin size was 250 m.

The strength of U_{max} was evaluated as a percentage of the MBL wind speed. The mean was found to be 19% higher than the MBL with 92% of the population of U_{max}/MBL values were below 1.25. However, outliers approached values 50% greater than the MBL. The ratio increased with the height of the wind maximum, as larger deviations from the MBL were found typically at higher altitudes. The ratio also generally increased for larger radii. The larger departures from the MBL at larger radii could be a result of sondes falling through convective elements associated with outer-rainbands which produced large perturbations from the MBL at radii well removed from the radius of maximum winds (RMW).

Low-level wind maxima were also examined in a storm-relative framework to evaluate any radial or azimuthal dependence. GPS sondes were stratified into storm-relative azimuth sectors: right-side: 20-150˚; rear: 150- 240˚; left-front: 240-20˚, as shown in Figure 4. The GPS sondes contained in the dataset appeared to be relatively evenly distributed across the range of storm-relative azimuths. There was an obvious bias radially, as sondes are often dropped with the intent to sample the strongest winds. Therefore there are a substantial number of observations within 100 km radii. As the figured showed, GPS sondes with a wind maximum below 200 km were confined to within 50 km radius. Only 10 sondes were found outside 50 km that contained a wind maximum below 200 m. Sondes with a maximum below 500 m were found in all sectors and exhibited little radial dependence. The rear sector exhibited the highest percentage of sondes with a wind maximum below 500 m and 200 m; however, when sondes with an MBL of less than 34 ms^{-1} were removed from the analysis, the results differed somewhat. Wind maxima below 500 m showed a preference for the right-side sector. The rear sector contained a substantial number of sondes with a wind maximum below 200 m from MBL wind speeds less than 34 ms^{-1}. The right-side sector appeared to be a favored location for wind maxima below 200 m for high MBL groups. It is noted that secondary wind maxima which do not contain the peak wind speed from the profile could alter the results.

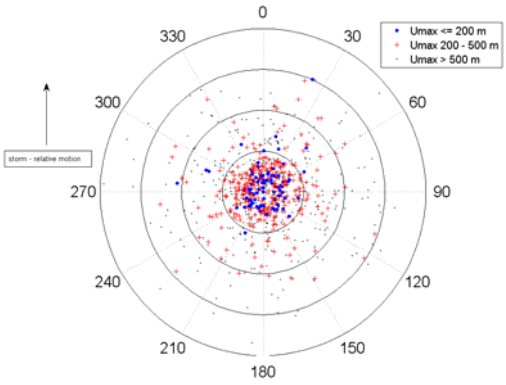

Figure 4. Plot of the storm-relative locations of all GPS sondes used. Storm-relative azimuth shown in degrees (dashed). Sondes with a wind maximum below 200 m are shown in blue. Wind maxima between 200-500 m are shown in red. Wind maxima above 500 m are shown in black. Range rings (solid black) represent 50, 100, 150, and 200 km radii.

Each sonde was assigned a cyclone intensification scale group to allow for the evaluation of wind maxima dependence on the tropical cyclone intensity trend. The groups are shown in Table 1 as well as the number of sondes which fell into each category. Sondes were stratified by intensification category as well. The steady-state grouping exhibited the highest percentage of sondes with a wind speed maximum below 500 m (44%), shown in Table 2. The mean value of U_{max}/MBL was very similar for all groups, shown in Table 2. The standard deviation was smallest for the rapidly intensifying group at 0.11, where the other three groups ranged from 0.20 – 0.36. The altitude of the wind maximum decreased with increased MBL for all four groups, as was

described when all sondes were examined as a whole. The altitude of the wind maximum also varied greatly within each grouping.

Table 2. Summary of sondes within each intensification category (see Table 1).

Intensification Category	Number of sondes	% of sonde with Umax < 500 m	Mean Umax/ MBL
Weakening	289	40%	1.18
Steady-state	691	44%	1.18
Intensifying	200	38%	1.21
Rapidly Intensifying	89	36%	1.18

4. Analysis of GPS sondes with a maximum below 200 m

Low-level wind maxima below 200 m represent a substantial concern to high-rise structures along the immediate coastline. The log-law was used to estimate the peak wind speed observed in each GPS sonde profile which contained a maximum below 200 m. It is noted that this method stretches the validity of surface-layer similarity theory. The final sonde observation was used to extrapolate to the height of the observed wind maximum for roughness length values (Z_o) of 0.01 m and 0.03 m. The WL150 surface wind estimate (Franklin et al. 2003) was also tested using a roughness length of 0.01 m. The WL150 was used strictly as a layer mean and no adjustment for eyewall or outer-vortex was applied due to the large number of sondes.

As expected the log profile for open terrain roughness (Z_o=0.03 m) underestimated the peak wind speed, with a mean bias error of -4.1 ms^{-1}. The error resulted in a mean underestimation of the wind load at the jet height by 16%, given a mean surface wind speed of 50 ms^{-1}. The roughness estimate of 0.01 m resulted in a mean positive bias of 2.1 ms^{-1}. It should be noted that little is known regarding roughness conditions at the immediate coastline or in shoaling wave conditions. It is a reasonable assumption that the dataset is more representative of open-ocean conditions than conditions at the immediate shoreline. Also, the final sonde observation is not a good representation of a 10 m one-minute mean wind speed; however engineering applications utilize the three-second gust to evaluate effects on structures. It is unclear what the averaging time period a sonde observation represents. The WL150 surface wind estimate resulted in a mean bias error of -4.6 ms^{-1}, for a surface roughness value of 0.01 m. Although there is no evidence to support the roughness estimates used, it does provide a crude estimate of the performance of the log-law for open and marine exposures. The errors associated with the log profile extrapolations for individual sondes were smaller than expected but exhibited a large variance. However, when fitted to mean profiles it remained a quite robust method. The 40-49.99 ms^{-1} and 50-59.99 ms^{-1} MBL groups, containing only sondes with a maximum below 200 m, were used to compute mean profiles and associated log fits. The profiles and log fits are shown in Figure 5. The log fits exhibited R^2 values of 0.9 and RMS errors of less than 0.1. The fitted profiles suggested that for maxima below 200 m, the log profile is a good estimate of the mean wind. However, the estimated roughness lengths varied between the two MBL groups. It is unclear how changes in surface roughness impact the mean low-level jet profiles or individual sonde jet profiles but results from the modeling study presented by Kepert (2001) suggested that increased surface roughness would result in a stronger, yet higher jet feature.

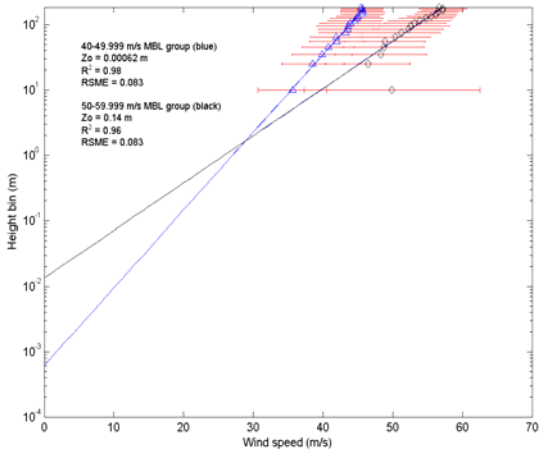

Figure 5. Mean profiles for the 40-49.99 ms^{-1} (blue) and the 50-59.99 ms^{-1} (black) MBL groups. The black line represents the least-squares fit for each MBL group. Error bars represent ± 1 σ from the mean. The 10 m height bin for the 50-59.999 ms^{-1} group did not contain at least 10 observations and was excluded from the fitted profile, although it is still included in the figure.

5. Characterizing tropical cyclone low-level jet features

In order to characterize tropical cyclone low-level jet features, suitable criteria for defining a low-level jet must be set. The maximum height to which an identified event could be classified a low-level jet was set at 1.5 km, similar to definitions of the classic nocturnal low-level jet (Bonner, 1968). It is a hypothesis of the study that low-level jet features represent a phenomenon which is not strictly a turbulent gust superimposed upon the mean wind profile. Given a mean wind profile, the jet structure is easily identified as a relatively weak but clear maximum (Franklin et al. 2003; Powell et al. 2003). Powell et al. (2003) showed a broad maximum where the wind speed exceeded the MBL between 200 and 1000 m. Individual dropsonde profiles indicate a more complex structure, which creates difficulty in distinguishing between a small-scale gust, transient feature, and a quasi-steady phenomenon representative of larger scales of motion.

The dataset previously described was altered for the next stage of analyses. GPS sondes which had missing wind or height data for more than two consecutive observations between 1500 and 100 m were excluded. The sondes were also grouped by 5 ms^{-1} MBL bin sizes opposed to 10 ms^{-1} used previously. However, the 80-89 ms^{-1} group was not altered due to the small number of sondes (15) which were contained within the group.

Individual sonde observations present a challenge to distinguish scales of motion as local maxima and minima are relatively common. It is also difficult to evaluate the temporal scales in which a sonde observation represents. The 5-s low-pass filter applied to sonde profiles during processing gives a cutoff vertical wavelength of approximately 50 m. Sonde data used in this study were not filtered further. The problem of identifying jet features is analogous to the identification of updrafts and downdrafts in tropical convection described by LeMone and Zipser (1980). A primary difference is that the sonde wind speed is not representative of a zero mean process; however this study will examine it as a perturbation from a layer-mean wind or the mean profile of a grouping of sondes stratified by MBL.

In an effort to evaluate sonde wind speed observations as a perturbation from a mean value, continuous layers where the wind speed exceeded the MBL wind speed were examined. A frequency distribution of layer depths is shown in Figure 6. The mean value was found to be 231 m; however the standard deviation was quite large, 276 m. The largest depths (> 900 m) depths were all found within MBL groups less than 35 ms^{-1}. The peak wind speed within each layer (U_{peak}) was identified and normalized to the MBL. The mean value was found to be 1.085, with a maximum of 1.38.

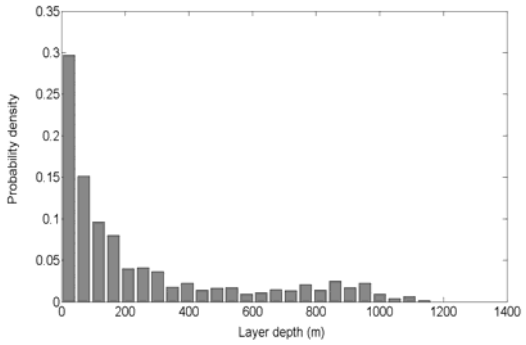

Figure 6. Frequency distribution of continuous layers where the instantaneous wind speed exceeded the MBL. Bin spacing was 45 m.

For the purposes of the presented study, a low-level jet will be identified as a continuous layer where the wind speed exceeded the MBL over a vertical depth of 75 m, which was found to be the 45% level of the distribution of layers where the wind speed exceeded the MBL (Figure 6). In similar fashion to LeMone and Zipser (1980), jet-cores were also identified in an effort to identify the strongest perturbations from the MBL. Cores were defined as peaks within jet features where U_{peak}/MBL exceeded 1.09, with no vertical depth requirement. This was representative of the 75th percentile of the of the U_{peak}/MBL distribution. Although somewhat arbitrary, the criteria were arrived at through substantial trial and error and captured secondary wind speed maxima, which occurred below the absolute maximum wind, quite well. The secondary jet feature appeared to be relatively common within a small number of individual sonde profiles subjectively examined. It is noted that the criteria for the jet event may result in a bias toward jets found below 500 m. Given the weakening pressure gradient with height

found in tropical cyclones, lower wind speeds would be expected to be found as altitude increases, therefore the MBL based criteria may not be able to capture jet-like structures at higher altitudes, or the criteria could underestimate the depth of the jet layer. However, the focus of this study is primarily on the lowest events which would have the potential to affect high-rise structures if they were to be found at landfall. The large number of sondes suggested that relatively simple criteria would be appropriate and less computationally expensive. Jets will be represented by their layer-mean value in future analyses, while cores will be identified by the peak wind speed within the occupied vertical layer. The median height of the jet layer will be used to describe the jet height. Jet events and their associated cores may or may not contain the maximum wind speed from the sonde profile and individual jets may contain multiple cores. Figure 7 provides an example of a sonde profile containing a jet and associated core.

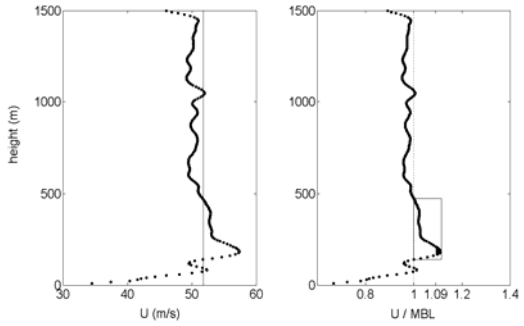

Figure 7. GPS sonde profile which exhibited a jet feature and jet-core. The wind profile is shown on the left. The normalized profile is shown on the right. Outlined is the jet layer. The jet core is the shaded region. The vertical line indicates the MBL.

The jet criteria identified 747 low-level jet events from a total of 1268 sondes. There were sondes which contained multiple jet events which resulted in a total of 511 sondes containing at least one jet event, approximately 40% of the dataset. Of the jet events identified, the maximum wind speed within the jet layer met the criteria for a jet-core in 391 of the events. The mean height of the jet layer was found to be 410 m, which is quite similar to the height of the wind maximum from mean profiles shown by Powell et al. (2003), Franklin et al. (2003), as well as modeling studies by Kepert (2001) and Kepert and Wang (2001). The frequency distribution of the jet layer height is shown in Figure 8 along with the distribution of the height of the jet layer wind maximum. Interestingly, the wind maximum within the jet layer exhibited a much lower mean altitude, 257 m. The result suggested that the wind maximum or jet-core (when criterion was met) was found within the lower portion of the jet layer. Also, 60% of the jet cores were found below 200 m, with 90% of the events found below 500 m. Conceptually, the turbulent kinetic energy profile found in tropical cyclones should decrease with increasing height; therefore the flow would be more turbulent at lower altitudes; however, there was little relation found between the peak wind speed from the jet layer and height, shown in Figure 9.

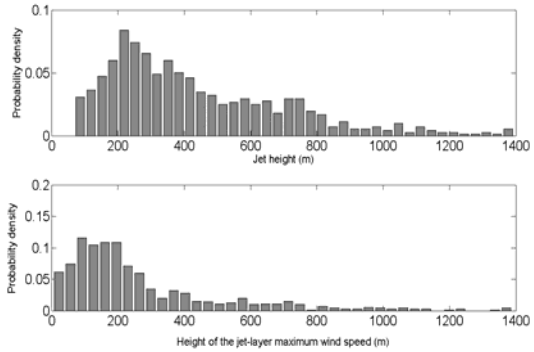

Figure 8. Frequency distribution of the jet layer height (top). Frequency distribution of the height of the maximum wind speed within each jet layer (bottom). Bin spacing was 35 m.

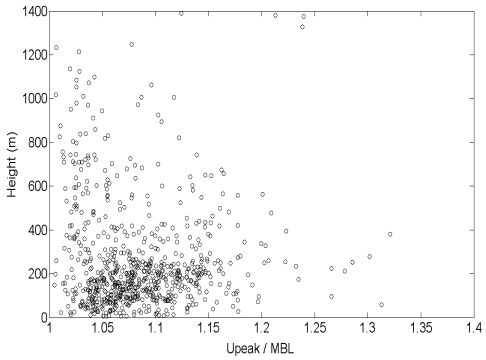

Figure 9. Jet layer-peak wind speed (ms^{-1}) normalized by MBL from each jet event plotted against the height (m) of the jet peak wind speed.

The jet events were examined in a storm-relative radial and azimuthal framework to examine favored locations of jet occurrence. Similar to the results previously described, jet events with a height below 200 m were concentrated at smaller radii; however the jet events identified exhibited a higher variance. Of the events which were found below 200 m, 60% were within 50 km radius. Jet events were identified in all sectors, shown in Figure 10. The differences between Figures 4 and 10 could be do to maxima at very low altitudes (< 75 m) being excluded from the jet criteria as the peak wind speed was very likely near the final sonde observation. Also secondary maxima were identified as jet events associated with larger radii. Jet cores were also examined in this fashion, shown in Figure 11. Jet cores below 200 m showed a preference for radii less than 50 km; however they were also found at greater radii. Only 7% of the jet cores were located above 500 m. The result was expected given the potential bias previously described for events at lower altitudes.

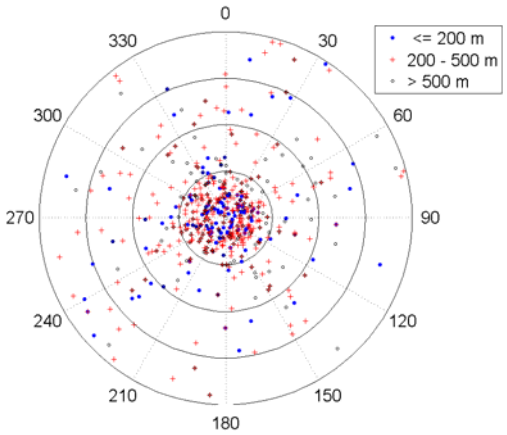

Figure 10. Storm-relative plot of all identified jet features. Jets found below 200 m are identified by blue stars. Jets between 200-500 m are identified in red. Jets located above 500 m are shown in black. Range rings (solid) represent 50, 100, 150, and 200 km radii. Storm-relative azimuth (dashed) shown in degrees.

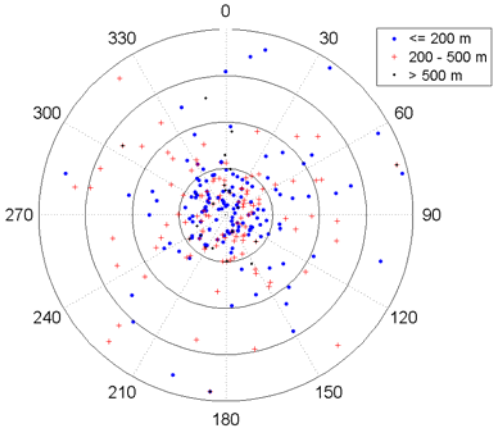

Figure 11. Storm-relative plot of all identified jet-cores. Cores found below 200 m are identified in blue. Jets between 200-500 m are identified in red. Jets located above 500 m are shown in black. Range rings (solid) represent 50, 100, 150, and 200 km radii. Storm-relative azimuth (dashed) shown in degrees.

6. Future work

The identification of the scales of motion within a GPS dropwindsonde is quite difficult and further effort is required. The results could lead to improved criteria for identifying jets and jet-cores as the method presented here is quite simple. A possible method would be to

use a linear model such as the one presented by Kepert (2001) to produce mean profiles and to compute the perturbations from the modeled profiles from the observational data. Kepert (2006 Pt I and Pt II.) showed that the linear model is capable of representing the mean vertical wind profile reasonably well. However, given the large number of sondes used in this study, this method may be impractical. It is noted that the jet and jet core criteria may be altered significantly as this study moves forward.

Additional work will also focus on further characterization of the identified jet features and jet-cores. The log and power law profiles will be evaluated as well using a variety of surface roughness characterizations to gain an understanding if the jet features represent a potential threat to high-rise structures along the immediate shoreline. A stochastic modeling approach will be employed to simulate the effects of observed vertical wind profiles on high-rise structures. It is unclear if the observed profiles are capable of producing significant damage.

7. Acknowledgements

The authors would like to acknowledge NSF(DGE-0221688 IGERT) for supporting this study.

Also special thanks to NOAA/AOML Hurricane Research Division for providing the post-processed GPS sonde data and Russell St. Fleur at NOAA/AOML/HRD for additional assistance with the sonde data.

8. References

Bonner, W. D., 1968: Climatology of the low-level jet. *Mon. Wea. Rev*., **96**, 833-850.

DeMaria, M. and J. Kaplan, 1994: A Statistical hurricane intensity prediction scheme (SHIPS) for the Atlantic basin. *Wea. Forecasting*, **9**, 209-220.

DeMaria, M. and J. Kaplan, 1999: An Updated Statistical Hurricane Intensity Prediction Scheme (SHIPS) for the Atlantic and Eastern North Pacific Basins. *Wea. Forecasting*, **14**, 326-337.

Franklin, J.L., M.L. Black and K. Valde, 2003: GPS dropwindsonde profiles in hurricanes and their operational implications. *Wea. Forecasting*, **18**, 32-44**.**

Hock, T.F., and J.L. Franklin, 1999: The NCAR GPS dropwindsonde. *Bull. Amer. Meteor. Soc.*, **80**, 407-420.

Holliday,C.R., and A.H. Thompson, 1979: Climatological characteristics of rapidly intensifying typhoons. *Mon. Wea. Rev.*, **107**, 1022-1034.

Kepert, J.D., 2001: The dynamics of boundary layer jets within the tropical cyclone core. Part I: Linear theory. *J. Atmos. Sci.* **58**, 2469-2483.

Kepert, J.D. and Y. Wang, 2001: The dynamics of boundary layer jets within the tropical cyclone core. Part II: Non-linear enhancement. *J. Atmos. Sci.* **58**, 2469-2483.

Kepert, J.D., 2006: Observed boundary layer wind structure and balance in the hurricane core. Part I: Hurricane Georges. *J. Atmos. Sci.* **63**, 2169-2193.

Kepert, J.D., 2006: Observed boundary layer wind structure and balance in the hurricane core. Part II: Hurricane Georges. *J. Atmos. Sci.* **63**, 2194-2211.

LeMone, M.A. and E.J Zipser, 1980: Cumulonimbus vertical velocity events in GATE. Part I: Diameter, intensity and mass flux. *J. Atmos. Sci.*, **37**, 2444-2457.

Powell, M.D., P.J. Vickery, and T.A. Reinhold, 2003: Reduced drag coefficients for high wind speeds in tropical cyclones. *Nature*, **422**, 279-283.